ChemComm

Accepted Manuscript

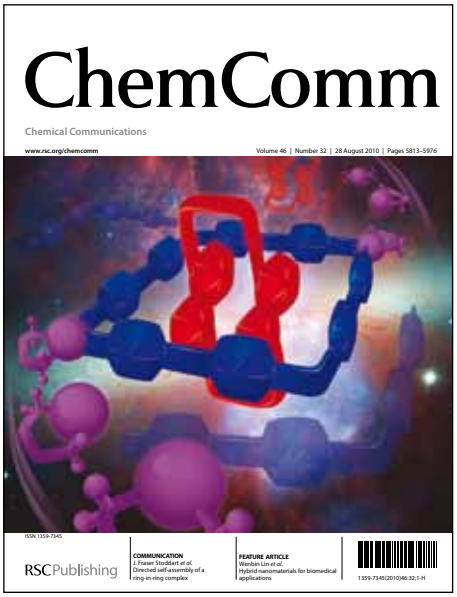

This is an *Accepted Manuscript*, which has been through the RSC Publishing peer review process and has been accepted for publication.

Accepted Manuscripts are published online shortly after acceptance, which is prior to technical editing, formatting and proof reading. This free service from RSC Publishing allows authors to make their results available to the community, in citable form, before publication of the edited article. This *Accepted Manuscript* will be replaced by the edited and formatted *Advance Article* as soon as this is available.

To cite this manuscript please use its permanent Digital Object Identifier (DOI®), which is identical for all formats of publication.

More information about *Accepted Manuscripts* can be found in the **Information for Authors**.

Please note that technical editing may introduce minor changes to the text and/or graphics contained in the manuscript submitted by the author(s) which may alter content, and that the standard **Terms & Conditions** and the **ethical guidelines** that apply to the journal are still applicable. In no event shall the RSC be held responsible for any errors or omissions in these *Accepted Manuscript* manuscripts or any consequences arising from the use of any information contained in them.

ChemComm

RSCPublishing

COMMUNICATION

Visible-Light-Driven Water Oxidation at a Polychromium-Oxo-Electrodeposited TiO_2 Electrode as a New Type of Earth-Abundant Photoanode

Cite this: DOI: 10.1039/xoxxoooooox

Received ooth January 2012,
Accepted ooth January 2012

DOI: 10.1039/xoxxoooooox

www.rsc.org/

Masashi Kajita,[a] Kenji Saito,[a] Naoto Abe,[a] Akinori Shoji,[a] Kazuki Matsubara,[a] Tatsuto Yui[a] and Masayuki Yagi[a,b]

A polychromium-oxo-deposited TiO_2 electrode was fabricated as an earth-abundant photoanode for visible-light-driven water oxidation by a simple electrochemical technique. The photoelectrocatalytic water oxidation could occur based on a specific interfacial charge transfer (IFCT) from a Cr^{III} to the TiO_2 conduction band.

An artificial photosynthetic device has been attracting much interest as one of the promising clean energy-providing systems in future.[1] Development of an efficient visible-light-driven anode for water oxidation to evolve O_2 is a key task to yield a breakthrough toward an artificial photosynthetic device. A great deal of effort has been devoted to develop it,[2] and n-type semiconductor electrodes such as α-Fe_2O_3,[2a] WO_3,[2b] $BiVO_4$,[2c] TaON,[2d] and Co-catalyst/ZnO[2e] have been reported as the possible visible-light-driven photoanode so far. A TiO_2 electrode is one of the most promising photoanodes due to its notable stability and a lot of accumulated knowledge. Although a TiO_2 electrode exhibits a UV light response, chemical adsorption of molecular dyes on the TiO_2 electrode surface provides a visible light response, as known especially in dye-sensitized solar cells.[3] Visible-light-assisted water oxidation was generated at the TiO_2 electrode by adsorbing a Ru dye linked with IrO_2 colloid as a water oxidation catalyst.[4] The internal quantum efficiency for water oxidation was reported to be ~0.9% at 450 nm under 0 mV vs Ag/AgCl[4a], and recently improved to be 2.3% (450 nm) by loading an electron mediator moiety on the IrO_2 colloid surface under the same conditions[4b]. The Ru dye-sensitization mechanism was extended to the other water oxidation catalyst systems of Mn-based catalysts[5] Ru complexes[6], and polyoxometalate[7] to establish light-driven O_2 production. However, from the viewpoint of industrial application in future, the use of earth-abundant elements and more simple methods were required for electrode preparation. Herein we fabricate a polychromium-oxo-deposited TiO_2 electrode as a precious element-free and visible-light-driven photoanode by a simple electrochemical technique based on the surface modification on a TiO_2 electrode. We report a unique electrode fabrication and photoanodic performance of visible-light-driven water oxidation.

A $Cr(NO_3)_3$ aqueous solution was pre-treated at -0.74 V vs. Ag/AgCl using a Pt electrode for 2h to cause the electrode preparation faster[8], and then an anatase TiO_2 electrode was cathodically polarized at the same potential in the pre-treated solution for 6 h to form the brown deposit on the TiO_2 electrode. The brown deposit was not formed using the aqueous solutions of $CrCl_3$, $Cr_2(SO_4)_3$ and $NaNO_3$ instead of $Cr(NO_3)_3$. To understand the specific electrodeposition from the $Cr(NO_3)_3$ solution, the UV-visible absorption and Raman spectra of the $Cr(NO_3)_3$ solution were measured. The UV-visible absorption spectral change of the $Cr(NO_3)_3$ solution during cathodic polarization displayed that an intense absorption band at 360 nm is generated with an isosbestic point at 540 nm in contrast to no spectral change in the cases using $CrCl_3$, $Cr_2(SO_4)_3$ and $NaNO_3$ (Figure S1). The Raman spectra of the $Cr(NO_3)_3$ solution after the 2 h electrolysis at -0.74 V vs. Ag/AgCl exhibited a peak at 900 cm^{-1}, in addition to 714 cm^{-1} and 1042 cm^{-1} for NO_3^- bending and symmetric stretching vibrations, respectively in a range of 600 ~ 1500 cm^{-1} (Figure S2). The peak at 900 cm^{-1} is assigned to the Cr-O vibration (890~904 cm^{-1}) of hydrated polychromium-oxo species.[9] The reduction of NO_3^- ions is known to generate OH^- according to eq. (1)[10], and it could be catalysed by Cr^{3+} ions as Lewis acid. Electrochemically formed OH^- are supposed to react with Cr^{3+} ions near the electrode surface to generate polychromium-oxo species in solution.

$$NO_3^- + H_2O + 2e^- \rightarrow NO_2 + 2OH^- \quad (1)$$

In cyclic voltammogram (CV) of the pre-treated solution using an anatase TiO_2 electrode, a reduction wave was given at -0.39 V vs. Ag/AgCl (Figure S3) with the brown deposit formed on the TiO_2 electrode surface. When an ITO or a Pt electrode was used for the same CV measurement, neither was the reduction peak at -0.39 V given, nor being the deposit observed on the electrode surface. This

Chemical Communications Accepted Manuscript

suggests the special electrodeposition of the brown deposit onto the TiO_2 surface.

The distinguishable difference in the SEM image was not observed between the surfaces of the TiO_2 electrode with brown deposit and the neat TiO_2 electrode (Figures S4a and b). Presumably, TiO_2 particles could be covered with a thin layer of small-size brown deposit (< 50 nm). The SEM image of its cross section indicated 8 μm of the film thickness of the TiO_2 electrode with brown deposit under the typical preparation conditions (Figure S4c). The geometric film thickness of a TiO_2 electrode was hardly changed before and after formation of brown deposition for SEM observation. Energy dispersive X-ray spectroscopic (EDS) data clearly showed the presence of chromium in the brown deposit, and the molar ratio of Ti : Cr was 1 : 0.49 on the electrode surface (Figure S5). The amount of deposited chromium was measured to be 6.4 μmol cm^{-2} under the typical preparation conditions using an inductively coupled plasma mass spectrometry technique. Chromium in the deposit was also indicated by the X-ray photoelectron spectroscopy spectra giving the peaks at 585.7 and 575.9 eV, assigned to Cr $2p_{1/2}$, $2p_{3/2}$, respectively (Figure S6). The binding energy (575.9 eV) agrees well with Cr^{III} binding to an oxygen atom (Cr_2O_3 : 576.0 eV), but with neither binding energies of the starting material ($Cr^{III}(NO_3)_3$: 577.3 eV), Cr^{III} hydroxide ($Cr(OH)_3$: 577.3 eV) nor Cr^{VI} oxide (CrO_3 : 578.9 eV). This suggests that Cr^{III}-oxo species are deposited on the electrode. The Raman spectrum of the brown deposited-TiO_2 surface showed a peak at 850 cm^{-1} in addition to three intensive peaks based on anatase TiO_2[11] in a range of 300 ~ 1000 cm^{-1}. (Figure S7). The Raman spectrum of Cr_2O_3 being chemically prepared exhibited two peaks at 550 and 850 cm^{-1}, the former of which can be assigned to Cr^{III}-O vibration energy of Cr_2O_3,[12] the latter being the dehydrated Cr-O vibration of chromium-oxo compounds[12b] (Figure S8). These XPS and Raman data suggest that the polychromium-oxo ($Cr^{III}{}_xO_y$) species with dehydrated Cr-O sites was electrodeposited on the electrode, but it is not neat Cr_2O_3 because of no peak around 550 cm^{-1} in the Raman spectrum (Figure S7). Raman spectral mapping analyses of the cross section of the film confirmed that the $Cr^{III}{}_xO_y$ species are uniformly deposited in the TiO_2 film from the ITO interface to the film surface (Figure S9).

The UV-visible absorption spectrum of the $Cr^{III}{}_xO_y$-deposited TiO_2 electrode exhibited a wide range of light absorption in a visible region of 400 ~ 800 nm (red solid line in Fig. 1A), in contrast to almost no visible absorption for the neat TiO_2 electrode (black solid line). It can be deconvoluted to at least three absorption bands. The first and second bands exhibit the absorption maximum at 600 and 460 nm, which can be assigned to d-d transitions from $^4A_{2g}$ to $^4T_{2g}$ and to $^4T_{1g}$, respectively[13]. The third one is at a shorter wavelength region than the others and provides an absorption edge at 560 nm. It could be assigned to the IFCT[14] from a 3d level of the deposited Cr^{III} to TiO_2 CB because the absorption edge at 560 nm (2.2 eV) is close to the transition energies from Cr^{III} 3d level to TiO_2 CB for rutile TiO_2 with Cr^{III}-doping (2.2 eV)[15] and grafting (2.1 eV).[14c] The $Cr^{III}{}_xO_y$-deposited TiO_2 electrode was compared with Cr_2O_3 deposited chemically on a TiO_2 substrate in the UV-visible diffuse reflectance spectrum (Figure S10). The difference between them can be interpreted by contribution of the third deconvoluted spectrum assigned to the IFCT transition in Fig 1A. This result is consistent with the specific electrodeposition onto the TiO_2 surface, as suggested in the CV data (Figure S3).

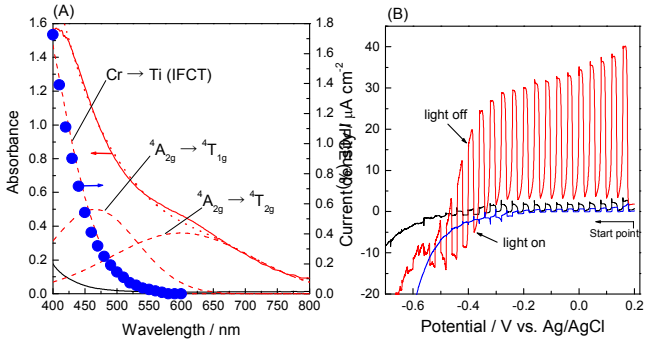

Fig.1 (A) UV-visible absorption spectra of the $Cr^{III}{}_xO_y$-deposited TiO_2 electrode (red solid line) and the neat TiO_2 electrode (black solid line). The red dashed lines are the deconvoluted bands of the former spectrum. The red dotted line is the spectrum simulated by the deconvoluted bands. Blue plots show the IPCE action spectrum of the $Cr^{III}{}_xO_y$-deposited TiO_2 electrode as measured at -0.2 V vs. Ag/AgCl in a 0.1 mol L^{-1} phosphate buffer (pH = 7.0). (B) I-V characteristics of the $Cr^{III}{}_xO_y$-deposited TiO_2 electrode (red line), the TiO_2 electrode with Cr_2O_3 deposited chemically (blue line), and the TiO_2 electrode (black line) in a 0.1 mol L^{-1} phosphate buffer (pH = 7.0) under monochromatic light irradiation (420 nm, 15.8 mW cm^{-2}).The potential sweep was started from 0.2 V.

Photoelectrochemical performance of the $Cr^{III}{}_xO_y$-deposited TiO_2 electrode was examined under monochromatic light (420 nm, 15.8 mW cm^{-2}) irradiation. The photoanodic current was significantly generated over -0.6 V vs. Ag/AgCl,[16] though it hardly generated on the TiO_2 electrode (Fig. 1B). It increased with an increase of the applied potential and reached 40 μA cm^{-2} at 0.2 V. In the similar experiment using the TiO_2 electrode with Cr_2O_3 deposited chemically, photocurrent was hardly generated similarly to the TiO_2 electrode[17] (Fig. 1B). This indicates that electrodeposited $Cr^{III}{}_xO_y$ species are important for the photoanodic current generation. The photocurrent increased linearly with increasing light intensity under the conditions (λ > 420 nm, 0 ~ 200 mW cm^{-2}) (Figure S11), suggesting that a photoexcitation process is involved in the photoanodic reaction. The action spectrum of incident photon-to-current efficiency (IPCE) measured at -0.2 V vs. Ag/AgCl is overlaid in Fig. 1A. The photocurrent was generated below 570 nm and increased with shortening wavelength to provide 1.7% of the IPCE value at 400 nm. The edge of the IPCE action spectrum corresponds well to that of the third deconvoluted band, indicating that the photocurrent could be based on IFCT photoexcitation.

Chemical Communications Accepted Manuscript

This journal is © The Royal Society of Chemistry 2012

Photoelectrolysis was conducted in a 0.1 mol L^{-1} phosphate buffer solution (pH = 7.0) at -0.2 V vs. Ag/AgCl under monochromatic light irradiation (420 nm, 15.8 mW cm^{-2}). For TiO_2 electrode, the current value during the photoelectrolysis was 0.19 ~ 0.08 μA cm^{-2}, and O_2 was not evolved during the 1 h catalysis. The photocurrent density of 42 μA cm^{-2} was generated at the initial stage, though it decreased to 7 μA cm^{-2} (17%) during the 1 hour photoelectrolysis (total charge 50.7 mC) using the $Cr^{III}_xO_y$-deposited TiO_2 electrode (Figure S12(A)). The gas in a headspace of the photoelectrochemical cell was analysed either by an optical O_2 sensor during the photoelectrolysis (Figure S12(B)) or by a gas chromatograph after photoelectrolysis. The amount of O_2 evolved was 0.12 μmol cm^{-2}, corresponding to Faradaic efficiency of 94%. O_2 evolution was observed over -0.45 V vs. Ag/AgCl. (Table S1) This result demonstrates that water is oxidized to O_2 by visible light. Initial internal quantum efficiency for oxygen evolution (Φ_{O2}) was 0.91% at 420 nm and -0.2 V vs Ag/AgCl. The UV-visible spectroscopic and EDS data corroborates that the $Cr^{III}_xO_y$-deposited TiO_2 electrode is unchanged before and after the photoelectrolysis (Figure S13 and S14). The decrease of the photocurrent density during the photoelectrolysis could be explained by accumulation of photogenerated holes, most possibly due to either slow hole diffusion in the $Cr^{III}_xO_y$ layer to the surface or slow water oxidation at the surface. The hole accumulation is supported by the repetitively-scanned CVs of the electrode after the photoelectrolysis with the monochromatic light irradiated (Figure S15). The large cathodic current was observed below -0.4 V vs. Ag/AgCl in the first scan cycle (dashed line) due to consumption of the hole accumulated, followed by the photoanodic current at 0.4 V regenerating after the second scan cycle. (inset of Figure S15) The photoanodic current recovered to 90% of that observed before the photoelectrolysis by the five-repetitive potential scan from 0.4V to -1.0V. To conclude, the electron transfer for visible-light-driven water oxidation is shown in Fig 2. When the visible light is irradiated to the $Cr^{III}_xO_y$-deposited TiO_2 electrode, the IFCT transition from a Cr 3d level of deposited $Cr^{III}_xO_y$ to TiO_2 CB could be induced. The generated holes could oxidize water to evolve O_2 on the Cr 3d level, the injected electrons to CB reducing H^+ to H_2 at the counter electrode (GC detected).

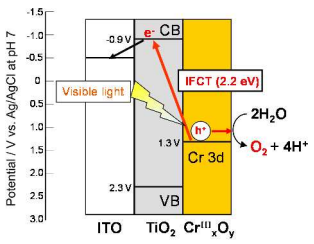

Fig. 2 Illustration of electron transfer proposed for visible-light-derived water oxidation on a $Cr^{III}_xO_y$-deposited TiO_2 electrode. VB and CB are a valence band and conduction band, respectively. Red arrow shows interfacial charge transfer (IFCT) from a Cr^{III} 3d level of the deposited $Cr^{III}_xO_y$ layer to TiO_2 CB.

Notes and references

[a] Department of Materials Science and Technology, Faculty of Engineering, Niigata University, 8050 Ikarashi-2, Niigata 950-2181, Japan. E-mail: yagi@eng.niigata-u.ac.jp; Fax: +81-25-262-6790; Tel: +81-25-262-6790
[b] PRESTO, Japan Science and Technology Agency, 4-1-8 Honcho, Kawaguchi, Saitama 332-0012, Japan

Electronic Supplementary Information (ESI) available: Experimental details, characterization data of the pre-treated solution and the electrode. See DOI: 10.1039/c000000x/

1. a) A. J. Bard and M. A. Fox, Acc. Chem. Res., 1995, 28, 141-145; b) W. J. Youngblood, S.-H. A. Lee, K. Maeda and T. E. Mallouk, Acc. Chem. Res., 2009, 42, 1966-1973; c) H. Yamazaki, A. Shouji, M. Kajita and M. Yagi, Coord. Chem. Rev., 2010, 254, 2483-2491.
2. a) A. Kay, I. Cesar and M. Gratzel, J. Am. Chem. Soc., 2006, 128, 15714-15721; b) C. Santato, M. Ulmann and J. Augustynski, J. Phys. Chem. B, 2001, 105, 936-940; c) K. Sayama, A. Nomura, Z. Zou, R. Abe, Y. Abe and H. Arakawa, Chem. Commun., 2003, 2908-2909; d) R. Abe, M. Higashi and K. Domen, J. Am. Chem. Soc., 2010, 132, 11828-11829; e) E. M. P. Steinmiller and K.-S. Choi, Proc. Natl. Acad. Sci. U. S. A., 2009, 106, 20633-20636.
3. a) B. O'Regan and M. Gratzel, Nature, 1991, 353, 737-740; b) A. Yella, H.-W. Lee, H. N. Tsao, C. Yi, A. K. Chandiran, M. K. Nazeeruddin, E. W.-G. Diau, C.-Y. Yeh, S. M. Zakeeruddin and M. Graetzel, Science, 2011 334 629-634
4. a) W. J. Youngblood, S.-H. A. Lee, Y. Kobayashi, E. A. Hernandez-Pagan, P. G. Hoertz, T. A. Moore, A. L. Moore, D. Gust and T. E. Mallouk, J. Am. Chem. Soc., 2009, 131, 926-927; b) Y. Zhao, J. R. Swierk, J. D. Megiatto, B. Sherman, W. J. Youngblood, D. Qin, D. M. Lentz, A. L. Moore, T. A. Moore, D. Gust and T. E. Mallouk, Proc. Natl. Acad. Sci. U. S. A., 2012.
5. R. Brimblecombe, A. Koo, G. C. Dismukes, G. F. Swiegers and L. Spiccia, J. Am. Chem. Soc., 2010, 132, 2892-2894.
6. a) L. Li, L. Duan, Y. Xu, M. Gorlov, A. Hagfeldt and L. Sun, Chem Commun, 2010, 46, 7307-7309; b) Y. Gao, X. Ding, J. Liu, L. Wang, Z. Lu, L. Li and L. Sun, J Am Chem Soc, 2013, 135, 4219-4222.
7. a) M. Orlandi, R. Argazzi, A. Sartorel, M. Carraro, G. Scorrano, M. Bonchio and F. Scandola, Chem. Commun., 2010, 46, 3152-3154; b) X. Xiang, J. Fielden, W. Rodríguez-Córdoba, Z. Huang, N. Zhang, Z. Luo, D. G. Musaev, T. Lian and C. L. Hill, J. Phys. Chem. C, 2013, 117, 918-926.
8. The similar electrode was prepared for 12 h without the pre-treatment.
9. a) D. Shee and A. Sayari, Appl. Catal., A, 2010, 389, 155-164; b) B. M. Weckhuysen, I. E. Wachs and R. A. Schoonheydt, Chem. Rev., 1996, 96, 3327-3350; c) F. C. Marques, M. C. Canela and A. M. Stumbo, Catal. Today, 2008, 133-135, 594-599.
10. X. H. Xia, J. P. Tu, J. Zhang, J. Y. Xiang, X. L. Wang and X. B. Zhao, Acs Appl Mater Inter, 2010, 2, 186-192.
11. T. Ohsaka, F. Izumi and Y. Fujiki, J. Raman Spectrosc., 1978, 7, 321-324.
12. a) T. V. Malleswara Rao, G. Deo, J.-M. Jehng and I. E. Wachs, Langmuir, 2004, 20, 7159-7165; b) B. M. Weckhuysen and I. E. Wachs, J. Phys. Chem. B, 1997, 101, 2793-2796; c) S. Khamlich, E. Manikandan, B. D. Ngom, J. Sithole, O. Nemraoui, I. Zorkani, R. McCrindle, N. Cingo and M. Maaza, J. Phys. Chem. Solids, 2011, 72, 714-718.
13. F. Cavani, M. Koutyrev, F. Trifiro, A. Bartolini, D. Ghisletti, R. Iezzi, A. Santucci and G. DelPiero, J. Catal., 1996, 158, 236-250.
14. a) N. S. Hush, J. Electroanal. Chem., 1999, 460, 5-29; b) C. Creutz, B. S. Brunschwig and N. Sutin, J. Phys. Chem. B, 2005, 109, 10251-10260; c) H. Irie, S. Miura, R. Nakamura and K. Hashimoto, Chem. Lett., 2008, 37, 252-253.
15. T. Ikeda, T. Nomoto, K. Eda, Y. Mizutani, H. Kato, A. Kudo and H. Onishi, J. Phys. Chem. C, 2008, 112, 1167-1173.

Chemical Communications Accepted Manuscript

16. The cathodic current below -0.4 V is ascribed to reduction of $Cr^{III}_xO_y$ deposited and H^+ reduction at the TiO_2 surface.
17. When the control sample is calcined at 500 °C, the photocurrent was hardly generated.

Chemical Communications Accepted Manuscript

This journal is © The Royal Society of Chemistry 2012